

# How Massive Single Stars End their Life

A. Heger

*Department of Astronomy and Astrophysics, Enrico Fermi Institute, The University of Chicago, 5640 S.  
Ellis Ave, Chicago, IL 60637*

[102sn.org](http://102sn.org)

C. L. Fryer

*Theoretical Astrophysics, MS B288, Los Alamos National Laboratories, Los Alamos, NM 87545  
fryer@lanl.gov*

S. E. Woosley

*Department of Astronomy and Astrophysics, University of California, Santa Cruz, CA 95064  
woosley@ucolick.org*

N. Langer

*Astronomical Institute, P.O. Box 80000, NL-3508 TA Utrecht, The Netherlands*

[N.Langer@astro.uu.nl](mailto:N.Langer@astro.uu.nl)

and

D. H. Hartmann

*Department of Physics and Astronomy, Clemson University, Clemson, SC 29634-0978  
hdietter@clemson.edu*

## ABSTRACT

How massive stars die – what sort of explosion and remnant each produces – depends chiefly on the masses of their helium cores and hydrogen envelopes at death. For single stars, stellar winds are the only means of mass loss, and these are chiefly a function of the metallicity of the star. We discuss how metallicity, and a simplified prescription for its effect on mass loss, affects the evolution and final fate of massive stars. We map, as a function of mass and metallicity, where black holes and neutron stars are likely to form and where different types of supernovae are produced. Integrating over an initial mass function, we derive the relative populations as a function of metallicity. Provided single stars rotate rapidly enough at death, we speculate upon stellar populations that might produce gamma-ray bursts and jet-driven supernovae.

*Subject headings:* massive stars, supernovae, stellar remnants, neutron stars, black holes, gamma-ray bursts, collapsars

## 1. Introduction

The fate of a massive star is governed chiefly by its mass and composition at birth and by the

history of its mass loss. For single stars, mass loss occurs as a result of stellar winds for which there exist semi-empirical estimates. Thus, within currently existing paradigms for the explosion, the

fate of a star of given initial mass and composition is determined (the Russell-Vogt theorem). If so, one can calculate realization frequencies for stellar explosions and remnants of various kinds and estimate how these might have evolved with time.

Such estimates are fraught with uncertainty. The litany of complications is long and requires discussion (§ 6). No two groups presently agree, in detail, on the final evolution of any massive star (including its explosion energy, remnant mass, and rotation rate) and the scaling of mass loss with metallicity during different evolutionary stages is widely debated. Still it is worthwhile to attempt an approximate table of histories. We would like to know, within the comparatively well understood domain of stars that do not experience mass exchange with a companion and for a particular set of assumptions regarding mass loss and explosion, what sort of supernova each star produces and what sort of bound remnant, if any, it leaves. If possible, we would also like some indication of which massive stars might make gamma-ray bursts.

In this paper we construct such a table of stellar fates and remnants. In § 2 we describe our assumptions regarding mass loss, explosion mechanism(s), and remnant properties, and in § 6 discuss the uncertainties. Section 4 delineates the sorts of stellar explosions and collapses we want to distinguish, and in § 5 we discuss the resulting realizations of different outcomes as a function of metallicity in the galaxy.

## 2. Assumptions

### 2.1. Stellar Models and Paradigms

The stellar models used in this paper were taken from Woosley & Weaver (1995); Heger & Woosley (2002b); Woosley et al. (2002) and Heger et al. (2003a). These papers treat the evolution of massive stars in the range 9 to  $300 M_{\odot}$  calculated without rotation from birth on the main sequence to death, either as iron-core collapse supernovae (helium core masses at death less than about  $65 M_{\odot}$ ) or pair instability supernovae (helium core masses at death greater than  $65 M_{\odot}$  and up to about  $135 M_{\odot}$ ). The effects of mass loss were included in those studies as discussed in § 2.2.

We shall presume here that the explosion mech-

anism, however it may operate, and the remnant properties are determined by the mass of the helium core when the star dies. (Perhaps the carbon oxygen core mass is a better discriminant, but systematics of the two are very similar). As the mass of the helium core increases, so does its binding energy and entropy. Because of its higher entropy, a larger helium core also has, on the average, a larger iron core mass, and a shallower density gradient around that core (Woosley et al. 2002). Consequently such stars are harder to explode (Fryer 1999; Fryer & Kalogera 2001). Even in “successful” explosions where a strong outward shock is born, mass may later fall back onto a neutron star remnant turning it, within one day, into a black hole. We thus distinguish black holes that are produced promptly or “directly” from those made by fall back.

Fryer (1999) has estimated that the helium core mass where black hole formation by fall back ensues is about  $8 M_{\odot}$  (a  $\lesssim 25 M_{\odot}$  main sequence star) and that direct black hole formation occurs for helium cores over  $15 M_{\odot}$  ( $40 M_{\odot}$  main sequence star with no mass loss). These numbers are uncertain (§ 6.2), but are representative choices. It is assumed that a baryonic remnant mass of over  $2.0 M_{\odot}$  will produce a black hole.

While the helium core mass governs the explosion mechanism, the hydrogen envelope is largely responsible for determining the spectrum (at peak) and light curve of common Type II supernovae. Stars with massive hydrogen envelopes when they die will be Type IIP; low mass envelopes will give Type IIL and IIB; etc. (§ 4). An exception are supernovae of Types Ib and Ic whose light curves do depend sensitively on the helium core mass since all the hydrogen envelope has been removed. The light curves of Types IIB, Ib, Ic, and 87A-like explosions are also sensitive to the amount of  $^{56}\text{Ni}$  made in the explosion.

### 2.2. Mass loss

The principal physics connecting the final evolution of a star to its metallicity is its mass loss. Low metallicity stars have less mass loss and have bigger helium cores and hydrogen envelopes when they die. To a lesser extent, metallicity also affects whether the presupernova star is a red or blue supergiant (Langer & Maeder 1995).

For main sequence stars and red supergiants the mass loss rates employed in the studies cited above were taken from Nieuwenhuijzen & de Jager (1990). For Wolf-Rayet stars, a mass-dependent mass loss rate (Langer 1989) was assumed using the scaling law established by Brown (1997); Wellstein & Langer (1999), but lowered by a factor 3 (Hamann & Koesterke 1998). Wind-driven mass loss is believed to be metallicity dependent and a scaling law  $\propto \sqrt{Z}$  has been suggested for hot stars (Kudritzki 2000; Nugis & Lamers 2000). Woosley et al. (2002) assumed that the same scaling law holds for Wolf-Rayet stars (Vanbeveren 2002) and blue and red supergiants as well. “Metallicity” is assumed here to be the initial abundance of heavy elements, especially of iron, not the abundances of new heavy elements like carbon and oxygen in the atmospheres of WC and WO stars (§ 6.1).

In very massive stars above  $\sim 60 M_{\odot}$ , the epsilon mechanism for pulsational driven mass loss sets in and enhances the mass loss during central hydrogen burning. Opacity-driven pulsations also become important, if not dominant, at high metallicity (Baraffe et al. 2001). At very low metallicity on the other hand, Baraffe et al. (2001) have shown that primordial stars should not have significant mass loss due to pulsations. This suggests significant evolution in the mass loss of very massive stars with metallicity (Figs. 1–4).

### 3. Remnant Properties

Fig. 1 shows the expected remnant types as a function of mass and initial “metallicity” for the above assumptions. In preparing Fig. 1, it is assumed that stars below  $\sim 9 M_{\odot}$  do not form massive enough cores to collapse, that they end their lives as white dwarfs. Just above this mass lies a narrow range,  $\sim 9 - 10 M_{\odot}$ , where degenerate oxygen-neon cores are formed that either collapse due to electron capture (Barkat et al. 1974; Miyaji et al. 1980; Nomoto 1984; Habets 1986; Miyaji & Nomoto 1987; Nomoto 1987; Nomoto & Hashimoto 1988) and make a neutron star or lose their envelopes and make white dwarfs (Garcia-Berro & Iben 1994; Ritossa et al. 1996; Garcia-Berro et al. 1997; Iben et al. 1997; Ritossa et al. 1999). Above  $\sim 10 M_{\odot}$  core collapse is the only alternative.

Wherever this transition between white dwarf

formation and iron core collapse lies, it should depend very little on metallicity and thus appears as a vertical line in Fig. 1. At low metallicities, the boundaries for black hole formation are also defined entirely by the initial stellar mass since there is a one to one correspondence between initial stellar mass and final helium core mass.

For stars of higher metallicity, mass loss becomes increasingly important resulting in smaller helium cores for a given initial mass. If the star loses its entire hydrogen envelope (to the right of the green line in Figs. 1–4), its rate of mass loss increases significantly (e.g., Langer 1989; Hamann et al. 1995) producing much smaller helium cores at collapse. This effect underlies the abrupt change in the otherwise vertical boundaries between neutron star, fallback black hole and direct black hole formation. For very massive stars, the remnant of the collapsing star depends sensitively on the metallicity. Above  $40 M_{\odot}$ , low metallicity stars form black holes directly, while at higher metallicities black holes of smaller mass are produced by fall back until, ultimately, only neutron stars are made. Winds are assumed to be stronger in higher mass stars, so the metallicity at which these transitions occur decreases with mass. But beyond  $\sim 100 M_{\odot}$ , this limit may rise again due to high enough initial mass or the significant role of evolution phases with lower mass loss rates (e.g., a WNL phases; see Brown et al. 2001).

At low metallicities, there is also a range of masses for massive stars that leave behind no remnant whatsoever. These are the pair-instability supernovae. If the helium core exceeds  $\sim 65 M_{\odot}$ , corresponding to a  $\sim 140 M_{\odot}$  initial mass for stars without mass loss, the pulsational pair instability (Heger & Woosley 2002b) becomes so violent that the star is disrupted entirely. When the helium core mass at the end of central carbon burning exceeds  $\sim 135 M_{\odot}$  for non-rotating stars (initial mass of  $\sim 260 M_{\odot}$  without mass loss), photodisintegration in the center leads to collapse to a very massive black hole ( $\gtrsim 100 M_{\odot}$ ), once again forming a black hole directly (Fryer et al. 2001; Heger & Woosley 2002b). However, as the metallicity increases, mass loss shifts the regime of pair-instability supernovae to higher initial masses. At still higher metallicities, these supernovae do not occur at all (Baraffe et al. 2001) because the progenitor stars are pulsationally unstable.

## 4. Supernovae

### 4.1. Supernovae of Type IIp and IIL

It has long been recognized that massive stars produce supernovae (Baade & Zwicky 1938). In this paper, we assume the following progenitor properties for the different core collapse supernova types:

SN Type	pre-SN stellar structure
IIP ....	$\gtrsim 2M_{\odot}$ H envelope
IIL ....	$\lesssim 2M_{\odot}$ H envelope
Ib/c ....	no H envelope

The lower and upper limits of main sequence mass that will produce a successful supernova (“M-lower” and “M-upper”) — one with a strong outgoing shock still intact at the surface of the star — has long been debated. On the lower end, the limit is set by the heaviest star that will eject its envelope quiescently and produce a white dwarf. Estimates range from 6 to  $11 M_{\odot}$  with smaller values characteristic of calculations that employ with a large amount of convective overshoot mixing (Marigo et al. 1996; Chiosi 2000) and the upper limit determined by whether helium shell flashes can eject the envelope surrounding a neon-oxygen core in the same way they do for carbon-oxygen cores (§ 3). It may also slightly depend on metallicity (Cassisi & Castellani 1993). Here we will adopt  $9 M_{\odot}$  for M-lower.

The value of M-upper depends on details of the explosion mechanism and is even more uncertain (§ 6.2). Fryer & Kalogera (2001) estimate  $40 M_{\odot}$ , but calculations of explosion even in supernovae as light as  $15 M_{\odot}$  give widely varying results. It is likely that stars up to at least  $25 M_{\odot}$  do explode, by one means or another, in order that the heavy elements be produced in solar proportions. The number of stars between  $25$  and  $40 M_{\odot}$  is not large. Here we have taken what some may regard as a rather large value, M-upper equals  $40 M_{\odot}$  (Fig. 2).

For increasing metallicity mass loss reduces the hydrogen envelope at the time of core collapse. A small hydrogen envelope ( $\lesssim 2 M_{\odot}$ ) can't sustain a long plateau phase in the light curve, and

only Type IIL supernovae or, for very thin hydrogen layers, Type I Ib supernovae result (Barbon et al. 1979; Filippenko 1997). It is also necessary for Type IIL supernovae that the radius be large (Swartz et al. 1991) and helpful if the  $^{56}\text{Ni}$  mass is not too small. The minimum metallicity for Type IIL supernovae in single stars, is set by the requirement that the mass loss needs to be strong enough to remove enough of the hydrogen envelope (Fig. 2). In single stars Type IIL/b SNe are formed only in a thin strip where the hydrogen envelope is almost but not entirely lost. Gaskell (1992) finds that Type IIL supernovae are currently about 10% - 20% as frequent as Type IIP.

For increasing metallicity this domain shifts to lower initial mass. Below a certain minimum metallicity we do not expect Type IIL supernovae from single stars at all. Indeed, those stars that form at the lowest (possible) metallicities will be so massive that they frequently form black holes by fall back and have not very luminous supernovae. This will be particularly true if the stars explode as blue supergiants but lack radioactivity.

### 4.2. Type Ib and Ic Supernovae

A complication is that Type Ib/c SNe with masses above  $4-5 M_{\odot}$ , which may be the most common ones to come from single stars, also have dim displays even if they are still powerful explosions (Enzman & Woosley 1988), i.e., the progenitor stars' cores are not so massive that they encounter significant fallback. In this paper, we do not differentiate these types of supernovae from our set of normal supernovae. Our assumptions regarding the different types of supernovae are summarized in the table below:

Type Ib/c He core mass at explosion	explosion energy	display
$\gtrsim 15 M_{\odot}$	direct collapse	none <sup>†</sup>
$\sim 15 - 8 M_{\odot}$	weak	dim <sup>†</sup>
$\sim 8 - 5 M_{\odot}$	strong	possibly dim
$\lesssim 5 M_{\odot}$	strong	bright

<sup>†</sup>if not rotating

Clearly, mass loss is a key parameter and both high metallicities (and high initial masses) are required to produce Type Ib/c supernovae in single stars. Woosley et al. (2002) find that for solar metallicity the limit for non-rotating stars is  $\sim 34 M_{\odot}$ . These supernovae can be weak and their later fallback will produce BH remnants. As with the Type II black-hole forming supernovae, we anticipate that this fallback, in particular of the  $^{56}\text{Ni}$  lost this way, may weaken the brightness of the supernova display, similar to the case of weak Type II SNe.

#### 4.3. Nickel-deficient Supernovae

The light curve of most supernovae is a consequence of two energy sources - shock-deposited energy and radioactivity, especially the decay of  $^{56}\text{Ni}$  to  $^{56}\text{Fe}$ . There are cases however, where the radioactive component may be weak or absent. If the hydrogen envelope is still present, a bright supernova may still result with the brightness depending on the explosion energy (Popov 1993), but the light curve lacks the characteristic radioactive “tail” (e.g., Sollerman et al. 1998; Turatto et al. 1998; Benetti et al. 2002). If the hydrogen envelope is gone (Type Ib/c), the consequences for the light curve are more dramatic and the supernova may be for practical purposes invisible.

Four cases of nickel-deficient supernovae may be noted.

- 1) *Stars in the mass range 9 to  $11 M_{\odot}$ .* Such stars have steep density gradients at the edge of degenerate cores. The shock wave from core collapse heats very little material to greater than  $5 \times 10^9$  K and very little ( $\lesssim 0.01 M_{\odot}$ )  $^{56}\text{Ni}$  is ejected (Mayle & Wilson 1988)
- 2) *Stars which make  $^{56}\text{Ni}$  but where the  $^{56}\text{Ni}$  falls back into the remnant.* This occurs for more massive stars with the threshold mass dependent upon both the presupernova structure and the explosion mechanism and energy. The boundary here is somewhat fuzzy because of the operation of mixing in conjunction with fallback. The lower limit for this regime is probably slightly larger than that for BH formation by fallback, the

upper limit is where BHs are formed directly without initiating a supernova, i.e.,  $10 M_{\odot} \lesssim$  helium core mass  $\lesssim 15 M_{\odot}$  (stellar masses  $30 M_{\odot} \lesssim M \lesssim 40 M_{\odot}$  without mass loss).

- 3) *Pair-instability supernovae with helium core masses in the range 65 to  $\lesssim 85 M_{\odot}$ .* Pair-instability supernovae, which probably only existed in the early universe can have light curves ranging from very faint if they have lost their hydrogen envelopes and eject no  $^{56}\text{Ni}$  to exceptionally brilliant if the converse is true (helium core  $\gtrsim 100 M_{\odot}$ ; Heger & Woosley 2002b; Heger et al. 2002a).
- 4) *Pulsational pair-instability supernovae with helium core masses in the range  $\gtrsim 40$  to  $65 M_{\odot}$ .* This instability occurs after central carbon burning but before the collapse. Though each pulse can have up to several  $10^{51}$  erg, only the outer layers of the star are expelled and contain no  $^{56}\text{Ni}$  (see below).

#### 4.4. Pair-instability supernovae

Very massive stars ( $M \gtrsim 100 M_{\odot}$ ) still form in the present galaxy (Najarro & Figer 1998; Eikenberry et al. 2001), but above  $\approx 60 M_{\odot}$ , nuclear-powered and opacity driven pulsations occur that increase the mass loss ( $\epsilon$ - and  $\kappa$ -mechanisms). Recently, Baraffe et al. (2001) have shown that both mechanisms are suppressed in extreme Pop III stars. Therefore it seems reasonable to assume that at sufficiently low metallicity ( $Z \lesssim 10^{-4} Z_{\odot}$ ) very massive stars may retain most of their mass through the end of central helium burning, forming a massive helium core (Baraffe et al. 2001; Kudritzki 2002; Marigo et al. 2003).

For zero-metallicity stars above  $\sim 100 M_{\odot}$  (helium cores  $\gtrsim 42 M_{\odot}$ ; Woosley 1986; Chiosi 2000; Heger & Woosley 2002b) stars encounter the the pair instability after central carbon burning (e.g., Bond et al. 1984; Heger & Woosley 2002b). Between  $\sim 100 M_{\odot}$  and  $\sim 140 M_{\odot}$  (helium core mass  $\lesssim 65 M_{\odot}$ ) the instability results in violent pulsations but not complete disruption. The implosive burning is not energetic enough to explode the star. Depending on the mass of the star and the strength of the initial pulse, subsequent pulses follow after  $\lesssim 1$  yr to  $\gtrsim 10,000$  yr. These pulsations continue until the star has lost so much mass, or decreased in central entropy, that it no longer

encounters the pair instability before forming an iron core in hydrostatic equilibrium. Since the iron core mass is large and the entropy high, such star probably finally make black holes.

The typical energy of these pulses can reach a few  $10^{51}$  erg and easily expels the hydrogen envelope, which is only loosely bound, in the first pulse (Heger & Woosley 2002b) – when these stars finally collapse they are thus hydrogen-free. Subsequent pulses may eject the outer layers of the helium core as well. Though the kinetic energy of these pulses may be well in excess of normal supernovae, they are less bright since they lack any  $^{56}\text{Ni}$  or other radioactivities that could power an extended light curve. However, the collision of shells ejected by multiple pulses could lead to a bright display.

For stars between  $\sim 140$  and  $\sim 260 \text{ M}_\odot$  (helium cores of  $\sim 64$  to  $\sim 133 \text{ M}_\odot$ ) the pair-instability is violent enough to completely disrupt the star in the first pulse (Ober et al. 1983; Bond et al. 1984; Heger & Woosley 2002b). Explosion energies range from  $\sim 3 \times 10^{51}$  erg to  $\lesssim 10^{53}$  erg and the ejected  $^{56}\text{Ni}$  mass ranges from zero to  $\gtrsim 50 \text{ M}_\odot$  at the high-mass end (Heger & Woosley 2002b). Above  $\sim 260 \text{ M}_\odot$ , the stars directly collapse to a black hole (Fryer et al. 2001; Heger & Woosley 2002b). Rotation would of course affect these mass limits.

## 4.5. Very energetic and asymmetric supernovae

### 4.5.1. Jet-powered supernovae

A jet-driven supernova (JetSN) is a grossly asymmetric supernova in which most of the energy comes from bipolar outflow from a central object. Though such supernovae may occur in association with gamma-ray bursts (GRBs), not all jet-powered supernovae will have sufficiently relativistic ejecta to make such a hard display. The class of jet-powered supernovae is thus a broad one having GRB progenitors as a subset.

Jet-Driven supernovae can be formed with or without hydrogen envelopes (MacFadyen et al. 2001; Nomoto et al. 2002; Fig. 4). The hydrogen-free JetSNe are closely related to GRBs. Whether such stars produce JetSNe or GRBs (or both) depends upon the rotation and the explosion mechanism. Until we understand both better, we can

not distinguish between the two.

### 4.5.2. Gamma-ray bursts and collapsars

The currently favored model for the formation of gamma-ray bursts assumes that a narrowly beamed ( $\theta \lesssim 10^\circ$ ) highly relativistic jet ( $\Gamma > 100$ ) leaves a compact “engine” and produces  $\gamma$ -rays either by internal shocks or by running into some external medium (Frail et al. 2001). Currently two classes of GRBs are distinguished: long and short bursts (Fishman & Meegan 1995). It is assumed that the short class might originate from binary neutron stars (Eichler et al. 1989), the long class could be produced by the collapse of the core of a massive star (e.g., Popham et al. 1999). In the present work we adopt this assumption, focus on the long class of GRBs, and use “GRB” synonymous for this class.

The term “collapsar” is used to describe all massive stars whose cores collapse to black holes and which have sufficient angular momentum to form a disk. There are three possible varieties.

I collapsars that form black holes “directly” during the collapse of a massive core. Although the star collapses and initially forms a proto-neutron star, it is unable to launch a supernova shock and eventually (after  $\sim 1$  s) collapses to form a black hole (Woosley 1993; MacFadyen & Woosley 1999).

II collapsars that form black holes by fallback after an initial supernova shock has been launched (MacFadyen et al. 2001). The explosion is too weak to eject much of the star, and the subsequent fallback of material causes the neutron star in the core to collapse and form a black hole.

III collapsars which do not form proto-neutron stars at all, but instead quickly collapse into massive black holes which grow through accretion (Fryer et al. 2001). These collapsars lead to the formation of massive ( $\sim 300 \text{ M}_\odot$ ) black holes.

type	time-scale	energy budget	initial BH mass
I	short	low	small
II	long	low	small
III	long	high	large

The results can be summarized as:

- Type I and II collapsars without a hydrogen envelope can make ordinary GRBs, though those of Type II will tend to be longer.
- Type II and III collapsars without a hydrogen envelope – maybe even with – can make very long GRBs (in their rest frame).
- All three types can make bright jet-powered supernovae if a hydrogen envelope is present.

Though we have described them as GRB progenitors, collapsars probably produce a variety of outbursts from X-ray flashes to jet-driven supernovae. Calculations to reliably show which stars make GRBs as opposed to just black holes are presently lacking (though see Heger & Woosley 2002a). Here we will assume that collapsars are made by some subset of those stars that make black holes (Fig. 3).

It is agreed however, that collapsars can only form GRBs if the star has lost its hydrogen envelope prior to collapse. Mass loss depends both on the stellar mass and metallicity and as both increase, the star uncovers more and more of its hydrogen envelope. The green curve in Figs. 3 and 4 denotes the boundary between stars which retain some of their hydrogen envelope and those that lose all of their hydrogen through mass loss. Above  $\sim 30 M_{\odot}$ , mass loss from winds become important, and as the initial mass of the star increases, lower and lower metallicities are required to retain the hydrogen envelope. Between  $100 - 140 M_{\odot}$ , pulsational instabilities are able to drive off the hydrogen layers of the star, even at zero metallicities. This boundary, which determines where stars lose their hydrogen envelopes marks the lower bound for GRB producing collapsars. The upper bound is set by those stars that collapse to form black holes.

## 5. Stellar Populations

With our evaluation of the possible fates of massive stars from § 4, we estimate the distribution of compact remnants and of observable outbursts produced by these single stars. The results will be uncertain. Not only do the predictions depend sensitively on the regions outlined in Figs. 1–4,

but also on the initial mass function (IMF) and its evolution.

In Fig. 6, we plot the fraction of massive stars forming neutron stars (*solid line*) and black holes (*dotted line*) assuming a Salpeter IMF (Salpeter 1955). At low metallicities, roughly 20% of massive stars form black holes, and roughly 75% form neutron stars. Half of those black holes form through fallback, the other half through direct collapse. Only 4% of black holes form massive ( $>200 M_{\odot}$ ) black holes. 1% of massive stars form pair-instability supernovae (leaving behind no remnant whatsoever). As the metallicity increases, the fraction of stars producing black holes first increases slightly (as the pair-instability mechanism is shut off) and then decreases near solar metallicity as most massive stars lose so much mass that they collapse to form neutron stars instead of black holes. At these high metallicities, all black holes are formed through fallback. Note that direct collapse black holes are larger than fallback black holes and black holes will be larger, on average, at low metallicity. In addition, if the black hole kick mechanism is powered by the supernova explosion, direct black holes will not receive kicks and these large black holes will tend to have small spatial velocities.

There is increasing evidence that the IMF is more skewed toward massive stars (relative to a Salpeter IMF) at low metallicities (e.g., Bromm et al. 2001; Abel et al. 2002, 2000). To include these effects, we have used the IMF for Population III by Nakamura & Umemura (2001). The *thin lines* in Fig. 6 show the change in the distribution of black holes and neutron stars using the Nakamura & Umemura (2001) IMF with the following parameters:  $m_{p_1} = 1.5$ ,  $m_{p_2} = 50$ ,  $\kappa = 0.5$ ,  $\alpha = \beta = 1.35$  (see Nakamura & Umemura 2001 for details). We employ this IMF up to a metallicity that corresponds to the last occurrence of (non-pulsational) pair instability supernovae (Fig. 2). Note that at low metallicities, where the IMF is skewed toward massive stars, the fraction of massive stars that form black holes is nearly twice as large as that predicted by a Salpeter IMF. Most of these black holes are formed through direct collapse.

If the mass limit at which weak supernovae occur decreases from  $25 M_{\odot}$  down to  $20 M_{\odot}$ , the fraction of neutron stars and typical Type IIP super-

novae at low metallicities drops below 70 %. The fraction of stars that form weak IIp supernovae and black holes increases to compensate this decrease. Table 1 summarizes the population fractions for different assumptions for the IMF and for the lower limit of the stellar core mass (i.e., lower limit of the initial mass for hydrogen-covered stars) resulting in fallback black hole formation. As mentioned above, here we assume that this corresponds to the maximum stellar/core mass forming strong SNe.

In Panel A of Fig. 7, we show the distribution of Type II supernovae. Most ( $\sim 90\%$ ) single massive stars produce Type II SNe (*solid line*). Most of these produce normal Type IIP SNe (*dashed line*). Roughly 10 % of all massive stars produce weak Type IIP SNe (*dot-dashed line*). As the metallicity approaches solar, some fraction of massive stars will produce Type IIL SNe. In Panel B, we plot the Type Ib/c SNe distribution. Single stars will not produce Type Ib/c SNe until the metallicity gets large enough to drive strong winds. At first, most Type Ib/c SNe will be produced by “weak” explosions that form black holes by fallback (*dot-dashed line*), but as the metallicity rises, an increasing fraction of “strong” Ib/c SNe is produced (*long dashed line*). Pair-instability SNe only occur at low metallicities and, for our choice of IMF, both pulsational and non-pulsational pair instability supernovae each constitute only about 1 % of all massive stars. When using the IMF by Nakamura & Umemura (2001) the pair SNe rates increase by a factor  $\sim 3$  (*thin lines*). Note that in Panel B of Fig. 7 the pair SNe rate is scaled by a factor 10.

Fig. 8 shows the distribution of GRBs and JetSNe (explosions arising from collapsars). Since in the frame of the present paper we cannot well distinguish between GRBs and JetSNe and, lacking a better understanding of rotation, these rates are upper limits only. The solid line in Fig. 8 reflects the total fraction of massive, single stars that could produce GRBs or JetSNe. The dotted line denotes the fraction of massive stars that could produce GRBs. To produce GRBs, the massive star must lose all of its hydrogen envelope, but still collapse to form a black hole. Hence, there is a narrow window of metallicities which allow GRB production in single stars. Because pulsational instabilities are able to eject the hydrogen

envelope of stars even at zero metallicities, some GRBs could be formed at low metallicities. As in Fig. 6, the thin lines denote the differences caused by using the Nakamura & Umemura (2001) IMF at low metallicities.

To determine a distribution of evolutionary outcomes versus redshift, we not only need to know the metallicity dependence of stellar winds, but we also need to know the metal distribution and spread as a function of redshift. This cosmic age-metallicity relation is likely to have large spreads and a weak trend (Pei & Fall 1995), as is also the case for this relation within the Milky Way (Matteucci 2001; Pagel 1997). These dependencies are difficult to determine because on a more global galactic or cosmological scale metals may be redistributed so that, e.g., most of the metals even for low metallicity stars could be produced in stars of metallicity. However, to give a flavor of possible redshift effects, we assume that the metallicity axis in Figs. 1–4 is indeed logarithmic and use the metallicity redshift distribution assumed by Lloyd-Ronning et al. (2002): Pei et al. (1999) distribution versus redshift with a Gaussian spread using a  $1 - \sigma$  deviation set to 0.5 in the logarithm of the metallicity. With these assumptions we can determine the distribution of neutron stars (*thick solid line*), black holes (*thick dotted line*), Type II SNe (*thin solid line*), Type Ib/c SNe (*thin dotted line*), pair supernovae (*thin dashed line*) as a function of redshift (or look-back time; Fig. 9). This suggests a trend in the populations of massive star outcomes versus redshift.

## 6. Uncertainties and possible consequences

### 6.1. Uncertainties in mass loss

Our mass loss rates explicitly include only radiatively driven mass loss, though the exact nature of the Wolf Rayet star mass loss is unknown. We do not include pulsational ejection and similar eruptions or by excretion disks in rapidly rotating stars (“ $\Omega$ -limit”; Langer 1997). The magnitude of these mass loss mechanisms depends upon the composition of the star. For hot stars both the absolute value and the metallicity-dependence of wind-driven mass loss are reasonably well understood and theoretically modeled (Kudritzki 2000, 2002). For most of the other mass loss mechanisms and temperature and mass regimes, we have

insufficient observational data or theoretical mass loss models to make precise predictions of a massive star's destiny. This is one reason we do not give precise values for metallicity along the axes in Figs. 1 – 4.

Though there is general consensus that reducing the initial metallicity of a massive star will increase its mass when it dies, the scaling of mass loss with  $Z$  during different stages of the evolution is controversial. We have made the simplest possible assumption, that mass loss rates scale everywhere as the square root of initial metallicity, essentially as the square root of the iron abundance. This is almost certainly naive. Vink et al. (2001) argue for a scaling  $Z^{0.69}$  for stars with  $T_{\text{eff}} > 25,000 \text{ K}$  and  $Z^{0.64}$  for B-supergiants with  $T_{\text{eff}} < 25,000 \text{ K}$ . Nugis & Lamers (2000) argued for a  $Z^{0.5}$  scaling in WN and WC stars, but for WC stars at least they had in mind the abundance of carbon in the atmosphere of the star, not the initial metallicity. On theoretical grounds, Kudritzki (2002) discusses a universal scaling for mass loss in hot stars that goes at  $Z^{0.5}$  but which has a threshold below which the mass loss declines more sharply.

For red supergiants, even the mass loss at solar metallicity is not well determined. At higher stellar masses the mass loss from luminous blue variables and WR stars also constitutes a major source of uncertainty as do pulsationally-induced and rotationally-induced outflows (see above).

## 6.2. Uncertainty in the explosion mechanism

The mechanism whereby the collapse of the iron core in a massive star results in a strong explosion has been debated for decades. The current paradigm is based on a neutrino powered “hot bubble” formed just outside the young proto-neutron star, but even the validity of this paradigm is debated along with its specific predictions (Herant et al. 1994; Burrows et al. 1995; Janka & Mueller 1996; Mezzacappa et al. 1998). The role of rotation and magnetic fields is also contentious (Leblanc & Wilson 1970; Fryer & Heger 2000; Ardeljan et al. 2001; Wheeler et al. 2002; § 6.3).

Our intuition here has been guided by parametric surveys in which the explosion is simu-

lated using a piston. The numerous uncertainties are thus mapped into choices of the piston's location and motion. These parameters are constrained by the requirement that the explosion not eject too much neutron-rich material (hence a minimum mass interior to the piston) and that the kinetic energy of the explosion measured at infinity be  $10^{51} \text{ erg}$ . Though a single event, SN 1987A occurred for a representative helium core mass ( $6 M_{\odot}$ ) and had a measured kinetic energy at infinity of  $\sim 1 - 1.5 \times 10^{51} \text{ erg}$  (Woosley 1988; Arnett et al. 1989; Bethe & Pizzochero 1990). The requirement that supernovae typically make  $\sim 0.1 M_{\odot}$  of  $^{56}\text{Ni}$  also means that the piston cannot be situated too far out or produce too weak an explosion. There are also more subtle conditions - that the mass cut frequently occur in a location where past (successful) calculations of the explosion have found it, that the distribution of remnant masses resemble what is observed for neutron stars, that the integrated ensemble of abundances resemble Population I in our galaxy, and so on.

Fig. 5 shows the remnant masses for a survey of explosions in solar metallicity stars that neglects mass loss. The progenitor stars described in Woosley et al. (2002) were exploded using a piston located at the edge of the “iron core”. The iron core was defined by the location of an abrupt jump in the neutron excess (electron mole number =  $Y_e = 0.49$ ). A constant kinetic energy at infinity ( $1.2 \times 10^{51} \text{ erg}$ ) was assumed (see also Woosley & Weaver 1995). In fact, the explosion energy will probably vary with mass. Fryer (1999) calculates that the explosion energy will actually weaken as the mass of the helium core increases. Thus fall back could have an even earlier onset and more dramatic effects than Fig. 5 would suggest.

The apparent non-monotonic behavior in Fig. 5 is largely a consequence of the choice of where the piston was sited. The neutronized iron core may have a variable mass that depends on details of oxygen and silicon shell burning (Woosley et al. 2002). The density gradient around that core can also be highly variable. Thus enforcing a constant kinetic energy at infinity does not always lead to a predictable variation of remnant mass with initial mass. More recent unpublished calculations by Heger et al. (2003a), also of zero metallicity stars, place the piston at an entropy jump (dimensionless entropy  $S/N_A k_B = 4$ ) rather than a

$Y_e$  jump. This choice, which is more consistent with explosion models, assumes that an explosion develops when the accretion rate declines rapidly. The rapid decline is associated with the density (and entropy) discontinuity near the base of the oxygen burning shell. Such a prescription gives more nearly monotonic results and, in particular the bump around  $17 M_\odot$  in Fig. 5 is absent.

Nevertheless Fig. 5 does suggest that the lines separating black hole formation by fall back from neutron stars in Figs. 1 - 4 should be interpreted only as indicating trends. They may not be as smooth or as monotonic as indicated.

### 6.3. Uncertainty in the effects of rotation

Rotation can enhance the mass loss in stars and a spread in initial rotation can smear out the transitions between the different mass and metallicity regimes. We have not considered cases where rotationally enhanced mass loss might be important. In such cases the limiting mass for loss of the hydrogen envelope could be lowered and, at the same time, the mass of the helium core increased (Heger et al. 2000; Meynet & Maeder 2000). The higher mass loss would tend to lower the metallicity for divisions between Type II and Type Ib/c supernovae as well as the divisions between strong, weak and no supernova explosions. The higher helium core masses with increase the metallicity divisions between strong, weak, and no supernova explosions. The total change will depend on the competition of the larger helium core masses and enhanced mass loss rate.

If the core is rotating rapidly at collapse, rotation may also influence the explosion mechanism and especially the possibility of making a GRB. Also pair-creation supernovae could be significantly affected by rotation, in particular the lower mass limit for direct black hole formation (Glatzel et al. 1985; Stringfellow & Woosley 1988). Early calculations that followed angular momentum in massive stars (e.g., Kippenhahn & Thomas 1970; Kippenhahn et al. 1970; Endal & Sofia 1976, 1978; Tassoul 2000) all found sufficient angular momentum retained in the core to reach critical rotation (“break-up velocity”) before the final central burning phases. More recent calculations by Heger (1998); Heger et al. (2000) find presupernova core rotation rates in massive stars that would lead to sub-millisecond neutrons stars

just around break-up if angular momentum were conserved perfectly during the collapse. Calculations by Meynet & Maeder (1997); Maeder & Zahn (1998); Maeder & Meynet, priv. com. (2000) indicate core rotation rates after central helium burning similar to those found by Heger et al. (2000).

Recently Spruit (2002) has discussed a “dynamo” mechanism based on the interchange instability that allows the estimation of magnetic torques to be included in models for stellar evolution. Preliminary calculations by Heger et al. (2002b, 2003b) that include these torques find a presupernova angular momentum equivalent to 5 - 10 milliseconds – still somewhat faster than observed young pulsars, but too slow for collapsars. If the estimates of magnetic torques by Spruit (2002) are valid then single stars are unlikely to produce collapsars and rotation is probably not a factor in the explosion of common supernovae. Nevertheless, in Fig. 3 we indicate the regimes where the structure of the star, excluding the question of sufficient rotation, is favorable for collapsars and GRBs.

## 7. Conclusions and Observational Tests

We have described, qualitatively, the likely fates of single massive stars as a function of metallicity. Our results suggest various trends in the observations of these objects which may be subject to observational tests.

- Normal Type Ib/c SNe are not produced by single stars until the metallicity is well above solar. Otherwise the helium core mass at death is too large. This implies that most Type Ib/c SNe are produced in binary systems where the binary companion aids in removing the hydrogen envelope of the collapsing star.
- Although less extreme than Type Ib/c SNe, single stars also do not produce Type IIL SNe at low metallicities. Similar to Type Ib/c SNe, Type IIL SNe from single stars are probably “weak” SNe until the metallicity exceeds solar, also implying that Type IIL SNe are produced in binaries.
- If GRBs are produced by single star collapse (perhaps unlikely given the constraints on

angular momentum), single stars only make up a small subset of GRB progenitors at higher metallicities. It is more likely that binary systems form GRBs. Such systems will occur more frequently at low metallicities (Fryer et al. 1999).

- Jet-driven supernovae from single stars are likely to be much more common than GRBs from single stars.

It is difficult to make direct comparisons to observations without including binary stars in our analysis, but there are a number of constraints that should be considered. First, an increasing number of JetSNe and weak supernovae explosions are being discovered (Nakamura et al. 2001; Sollerman et al. 1998; Turatto et al. 1998). Although there is an observational bias against the discovery of weak supernovae and they are much dimmer than JetSNe, they may still dominate the sample of stars more massive than  $25 M_{\odot}$ . Clearly, good statistics (and correct analysis of the systematics) are necessary to determine the relative ratio of jet-driven and weak SNe. With such statistics, we may be able to place constraints on the rotation of massive stellar cores.

If the IMF becomes more top-heavy at low metallicity ( $\lesssim 10^{-4} Z_{\odot}$ ; Bromm et al. 2001; Schneider et al. 2002) the number of core collapse supernovae (mostly Type IIp) and GRBs (if occurring in single stars) should significantly increase at high redshift. If the current estimates of a characteristic mass of  $\sim 100 M_{\odot}$  for primordial stars (Bromm et al. 1999; Abel et al. 2002; Nakamura & Umemura 2001) is correct we should expect a large fraction of pair SNe and very massive black holes (or Type III collapsars) at zero metallicity, as well as an increase of massive black holes from stars in the  $60-140 M_{\odot}$  region.

We thank Bruno Leibundgut for discussions about supernova classifications and Thomas Janka, Ewald Müller, and Wolfgang Hillebrandt for many helpful conversations regarding the explosion mechanism. This research has been supported by the NSF (AST 02-06111), the SciDAC Program of the DOE (DE-FC02-01ER41176), the DOE ASCI Program (B347885). AH is supported in part by the Department of Energy under grant B341495 to the Center for Astrophysical Thermonuclear

Flashes at the University of Chicago and acknowledges supported by a Fermi Fellowship of the Enrico Fermi Institute at The University of Chicago. The work of CF was funded by a Feynman Fellowship at LANL.

## REFERENCES

- Abel, T., Bryan, G. L., & Norman, M. L. 2000, ApJ, 540, 39
- . 2002, Science, 295, 93
- Ardeljan, N. V., Bisnovatyi-Kogan, G. S., & Moiseenko, S. G. 2001, *Astrophysics and Space Science Supplement*, 276, 295
- Arnett, W. D., Bahcall, J. N., Kirshner, R. P., & Woosley, S. E. 1989, ARA&A, 27, 629
- Baade, W. & Zwicky, F. 1938, Phys. Rev., 45, 138
- Baraffe, I., Heger, A., & Woosley, S. E. 2001, ApJ, 550, 890
- Barbon, R., Ciatti, F., & Rosino, L. 1979, A&A, 72, 287
- Barkat, Z., Reiss, Y., & Rakavy, G. 1974, ApJ, 193, L21
- Benetti, S., Branch, D., Turatto, M., Cappellaro, E., Baron, E., Zampieri, L., Della Valle, M., & Pastorello, A. 2002, MNRAS, 336, 91
- Bethe, H. A. & Pizzochero, P. 1990, ApJ, 350, L33
- Bond, J. R., Arnett, W. D., & Carr, B. J. 1984, ApJ, 280, 825
- Bromm, V., Coppi, P. S., & Larson, R. B. 1999, ApJ, 527, L5
- Bromm, V., Ferrara, A., Coppi, P. S., & Larson, R. B. 2001, MNRAS, 328, 969
- Brown, G. E., Heger, A., Langer, N., Lee, C.-H., Wellstein, S., & Bethe, H. A. 2001, New Astronomy, 6, 457
- Brown, H. 1997, PhD thesis, Ludwig-Maximilians Universität München
- Burrows, A., Hayes, J., & Fryxell, B. A. 1995, ApJ, 450, 830
- Cassisi, S. & Castellani, V. 1993, ApJS, 88, 509

- Chiosi, C. 2000, in The First Stars. Proceedings of the MPA/ESO Workshop held at Garching, Germany, 4-6 August 1999. Achim Weiss, Tom G. Abel, Vanessa Hill (eds.). Springer, p.95, 95
- Eichler, D., Livio, M., Piran, T., & Schramm, D. N. 1989, *Nature*, 340, 126
- Eikenberry, S. S., Matthews, K., Garske, M. A., Hu, D., Jackson, M. A., Patel, S. G., Barry, D. J., Colonna, M. R., Houck, J. R., & Wilson, J. C. 2001, American Astronomical Society Meeting, 199, 0
- Endal, A. S. & Sofia, S. 1976, *ApJ*, 210, 184
- . 1978, *ApJ*, 220, 279
- Enzman, L. M. & Woosley, S. E. 1988, *ApJ*, 333, 754
- Filippenko, A. V. 1997, *ARA&A*, 35, 309
- Fishman, G. J. & Meegan, C. A. 1995, *ARA&A*, 33, 415
- Frail, D. A., Kulkarni, S. R., Sari, R., Djorgovski, S. G., Bloom, J. S., Galama, T. J., Reichart, D. E., Berger, E., Harrison, F. A., Price, P. A., Yost, S. A., Diercks, A., Goodrich, R. W., & Chaffee, F. 2001, *ApJ*, 562, L55
- Fryer, C. L. 1999, *ApJ*, 522, 413
- Fryer, C. L. & Heger, A. 2000, *ApJ*, 541, 1033
- Fryer, C. L. & Kalogera, V. 2001, *ApJ*, 554, 548
- Fryer, C. L., Woosley, S. E., & Hartmann, D. H. 1999, *ApJ*, 526, 152
- Fryer, C. L., Woosley, S. E., & Heger, A. 2001, *ApJ*, 550, 372
- Garcia-Berro, E. & Iben, I. 1994, *ApJ*, 434, 306
- Garcia-Berro, E., Ritossa, C., & Iben, I. J. 1997, *ApJ*, 485, 765
- Gaskell, C. M. 1992, *ApJ*, 389, L17
- Glatzel, W., Fricke, K. J., & El Eid, M. F. 1985, *A&A*, 149, 413
- Habets, G. M. H. J. 1986, *A&A*, 167, 61
- Hamann, W.-R. & Koesterke, L. 1998, *A&A*, 335, 1003
- Hamann, W.-R., Koesterke, L., & Wessolowski, U. 1995, *A&A*, 299, 151
- Heger, A. 1998, PhD thesis, Technische Universität München
- Heger, A., Langer, N., & Woosley, S. E. 2000, *ApJ*, 528, 368
- Heger, A. & Woosley, S. E. 2002a, in Woods Hole GRB Meeting, ed. R. Vanderspek, in press; astro-ph/0206005
- Heger, A. & Woosley, S. E. 2002b, *ApJ*, 567, 532
- Heger, A., Woosley, S. E., Baraffe, I., & Abel, T. 2002a, in From Twilight to Highlight: The Physics of Supernovae, ed. W. Hillebrandt & B. Leibundgut, ESO Astrophysics Symposia, ESO/MPA (Springer-Verlag), in press; astro-ph/0211063
- Heger, A., Woosley, S. E., & Hoffman, R. D. 2003a, *ApJ*, in preparation
- Heger, A., Woosley, S. E., & Langer, N. 2002b, in A Massive Star Odyssey, from Main Sequence to Supernova, ed. K. A. van der Hucht, A. Herrero, & C. Esteban, IAU Symposium No. 212, in press
- Heger, A., Woosley, S. E., & Spruit, H. C. 2003b, *ApJ*, in preparation
- Herant, M., Benz, W., Hix, W. R., Fryer, C. L., & Colgate, S. A. 1994, *ApJ*, 435, 339
- Iben, I. J., Ritossa, C., & Garcia-Berro, E. 1997, *ApJ*, 489, 772
- Janka, H.-T. & Mueller, E. 1996, *A&A*, 306, 167
- Kippenhahn, R., Meyer-Hofmeister, E., & Thomas, H. C. 1970, *A&A*, 5, 155
- Kippenhahn, R. & Thomas, H.-C. 1970, in IAU Colloq. 4: Stellar Rotation, 20
- Kudritzki, R. 2000, in The First Stars. Proceedings of the MPA/ESO Workshop held at Garching, Germany, 4-6 August 1999. Achim Weiss, Tom G. Abel, Vanessa Hill (eds.). Springer, 127
- Kudritzki, R. P. 2002, *ApJ*, 577, 389
- Langer, N. 1989, *A&A*, 220, 135

- Langer, N. 1997, in ASP Conf. Ser. 120: Luminous Blue Variables: Massive Stars in Transition, 83
- Langer, N. & Maeder, A. 1995, A&A, 295, 685
- Leblanc, J. M. & Wilson, J. R. 1970, ApJ, 161, 541
- Lloyd-Ronning, N. M., Fryer, C. L., & Ramirez-Ruiz, E. 2002, ApJ, 574, 554
- MacFadyen, A. I. & Woosley, S. E. 1999, ApJ, 524, 262
- MacFadyen, A. I., Woosley, S. E., & Heger, A. 2001, ApJ, 550, 410
- Maeder, A. & Zahn, J. 1998, A&A, 334, 1000
- Marigo, P., Bressan, A., & Chiosi, C. 1996, A&A, 313, 545
- Marigo, P., Chiosi, C., & Kudritzki, R.-P. 2003, A&A, in press; astro-ph/0212057
- Matteucci, F. 2001, in Galaxy Disks and Disk Galaxies, ed. J. Funes & E. Corsini
- Mayle, R. & Wilson, J. R. 1988, ApJ, 334, 909
- Meynet, G. & Maeder, A. 1997, A&A, 321, 465
- . 2000, A&A, 361, 101
- Mezzacappa, A., Calder, A. C., Bruenn, S. W., Blondin, J. M., Guidry, M. W., Strayer, M. R., & Umar, A. S. 1998, ApJ, 495, 911
- Miyaji, S. & Nomoto, K. 1987, ApJ, 318, 307
- Miyaji, S., Nomoto, K., Yokoi, K., & Sugimoto, D. 1980, PASJ, 32, 303
- Najarro, F. & Figer, D. F. 1998, Ap&SS, 263, 251
- Nakamura, F. & Umemura, M. 2001, ApJ, 548, 19
- Nakamura, T., Umeda, H., Iwamoto, K., Nomoto, K., Hashimoto, M., Hix, W. R., & Thielemann, F. 2001, ApJ, 555, 880
- Nieuwenhuijzen, H. & de Jager, C. 1990, A&A, 231, 134
- Nomoto, K. 1984, ApJ, 277, 791
- . 1987, ApJ, 322, 206
- Nomoto, K. & Hashimoto, M. 1988, Phys. Rep., 13
- Nomoto, K., Maeda, K., Umeda, H., Ohkubo, T., Deng, J., & Mazzali, P. 2002, in A Massive Star Odyssey, from Main Sequence to Supernova, ed. K. A. van der Hucht, A. Herrero, & C. Esteban, IAU Symposium No. 212, in press; astro-ph/0209064
- Nugis, T. & Lamers, H. J. G. L. M. 2000, A&A, 360, 227
- Ober, W. W., El Eid, M. F., & Fricke, K. J. 1983, A&A, 119, 61
- Pagel, B. E. J. 1997, Nucleosynthesis and Chemical Evolution of Galaxies (Cambridge Univ. Press)
- Pei, Y. C. & Fall, S. M. 1995, ApJ, 454, 69
- Pei, Y. C., Fall, S. M., & Hauser, M. G. 1999, ApJ, 522, 604
- Popham, R., Woosley, S. E., & Fryer, C. 1999, ApJ, 518, 356
- Popov, D. V. 1993, ApJ, 414, 712
- Ritossa, C., Garcia-Berro, E., & Iben, I. J. 1996, ApJ, 460, 489
- Ritossa, C., García-Berro, E., & Iben, I. J. 1999, ApJ, 515, 381
- Salpeter, E. E. 1955, ApJ, 121, 161
- Schneider, R., Ferrara, A., Natarajan, P., & Omukai, K. 2002, ApJ, 571, 30
- Sollerman, J., Cumming, R. J., & Lundqvist, P. 1998, ApJ, 493, 933
- Spruit, H. C. 2002, A&A, 381, 923
- Stringfellow, G. S. & Woosley, S. E. 1988, in The Origin and Distribution of the Elements, ed. G. J. Mathews (Singapore: World Scientific Press), 467
- Swartz, D. A., Wheeler, J. C., & Harkness, R. P. 1991, ApJ, 374, 266
- Tassoul, J.-L. 2000, Stellar Rotation (Cambridge Univ. Press)

Turatto, M., Mazzali, P. A., Young, T. R., Nomoto, K., Iwamoto, K., Benetti, S., Cappallaro, E., Danziger, I. J., de Mello, D. F., Phillips, M. M., Suntzeff, N. B., Clocchiatti, A., Piemonte, A., Leibundgut, B., Covarrubias, R., Maza, J., & Sollerman, J. 1998, ApJ, 498, L129

Vanbeveren, D. 2002, in The Influence of Binaries on Stellar Population Studies, ed. D. Vanbeveren, ASSL series (Dordrecht: Kluwer Academic Publishers), in press; astro-ph/0201110

Vink, J. S., de Koter, A., & Lamers, H. J. G. L. M. 2001, A&A, 369, 574

Wellstein, S. & Langer, N. 1999, A&A, 350, 148

Wheeler, J. C., Meier, D. L., & Wilson, J. R. 2002, ApJ, 568, 807

Woosley, S. E. 1986, in Saas-Fee Advanced Course 16: Nucleosynthesis and Chemical Evolution, 1

Woosley, S. E. 1988, ApJ, 330, 218

—. 1993, ApJ, 405, 273

Woosley, S. E., Heger, A., & Weaver, T. A. 2002, Reviews of Modern Physics, 74, 1015

Woosley, S. E. & Weaver, T. A. 1995, ApJS, 101, 181

Table 1: Remnant and supernova population yields for different metallicities, IMFs, and mass limits.

Object	Zero Metallicity				Solar Metallicity	
	high $M_{\text{FBH}}^{\text{lim}}$		low $M_{\text{FBH}}^{\text{lim}}$		high $M_{\text{FBH}}^{\text{lim}}$	low $M_{\text{FBH}}^{\text{lim}}$
	IMF <sub>Sal</sub>	IMF <sub>NU</sub>	IMF <sub>Sal</sub>	IMF <sub>NU</sub>	IMF <sub>Sal</sub>	IMF <sub>Sal</sub>
Remnants						
NS	75	56	66	50	87	75
BH	23	36	32	43	13	25
MBH	0.9	3.0	0.9	3.0	0	0
Supernovae						
IIP Strong	75	56	66	50	77	70
IIP Weak	12	8.9	21	16	0	6.9
IIL	0	0	0	0	6.4	6.4
Ib/c Strong	0	0	0	0	9.2	5.1
Ib/c Weak	0	0	0	0	7.6	12
Other Outbursts						
Puls. Pair	1.4	4.7	1.4	4.7	0	0
Pair SNe	1.4	4.6	1.4	4.6	0	0
Jet SNe	24	39	33	46	13	25
GRBs	1.4	3.4	1.4	4.7	7.8	12

NOTE: For solar metallicity we use the IMF by Salpeter (1955; IMF<sub>Sal</sub>), for zero metallicity we additionally supply the results for the IMF by Nakamura & Umemura (2001; IMF<sub>NU</sub>). We give the results two different lower mass limits for fallback black hole formation ( $M_{\text{FBH}}^{\text{lim}}$ ): *high* corresponds to  $25 M_{\odot}$  and *low* to  $20 M_{\odot}$  (Fryer 1999).

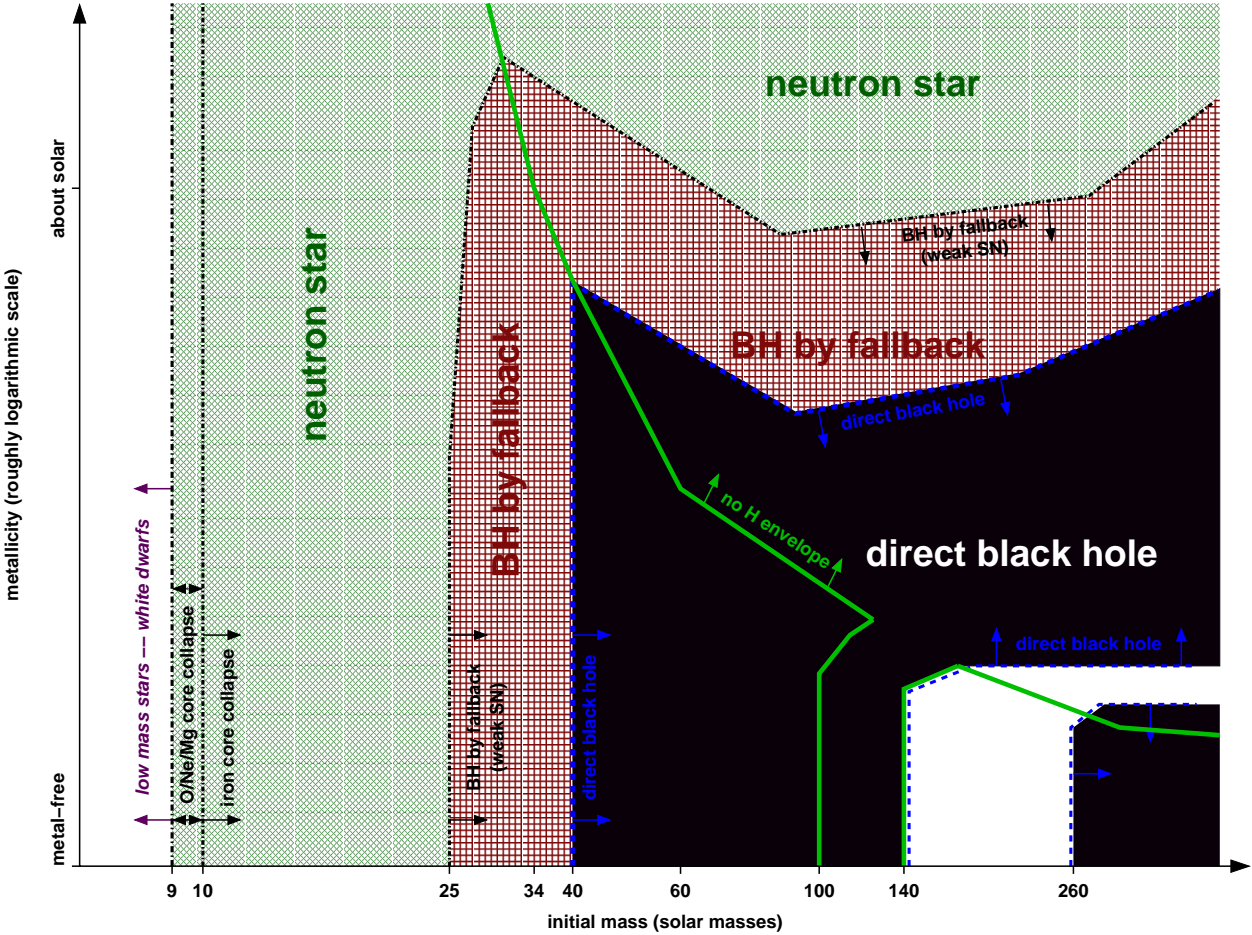


Fig. 1.— Remnants of massive single stars as a function of initial metallicity (y-axis; qualitatively) and initial mass (x-axis). The *thick green line* separates the regimes where the stars keep their hydrogen envelope (left and lower right) from those where the hydrogen envelope is lost (upper right and small strip at the bottom between 100 and 140  $M_{\odot}$ ). The *dashed blue line* indicates the border of the regime of direct black hole formation (*black*). This domain is interrupted by a strip of pair-instability supernovae that leave no remnant (*white*). Outside the direct black hole regime, at lower mass and higher metallicity, follows the regime of BH formation by fallback (*red cross hatching* and bordered by a *black dash-dotted line*). Outside of this, *green cross hatching* indicates the formation of neutron stars. The lowest-mass neutron stars may be made by O/Ne/Mg core collapse instead of iron core collapse (*vertical dash-dotted lines* at the left). At even lower mass, the cores do not collapse and only white dwarfs are made (*white strip* at the very left).

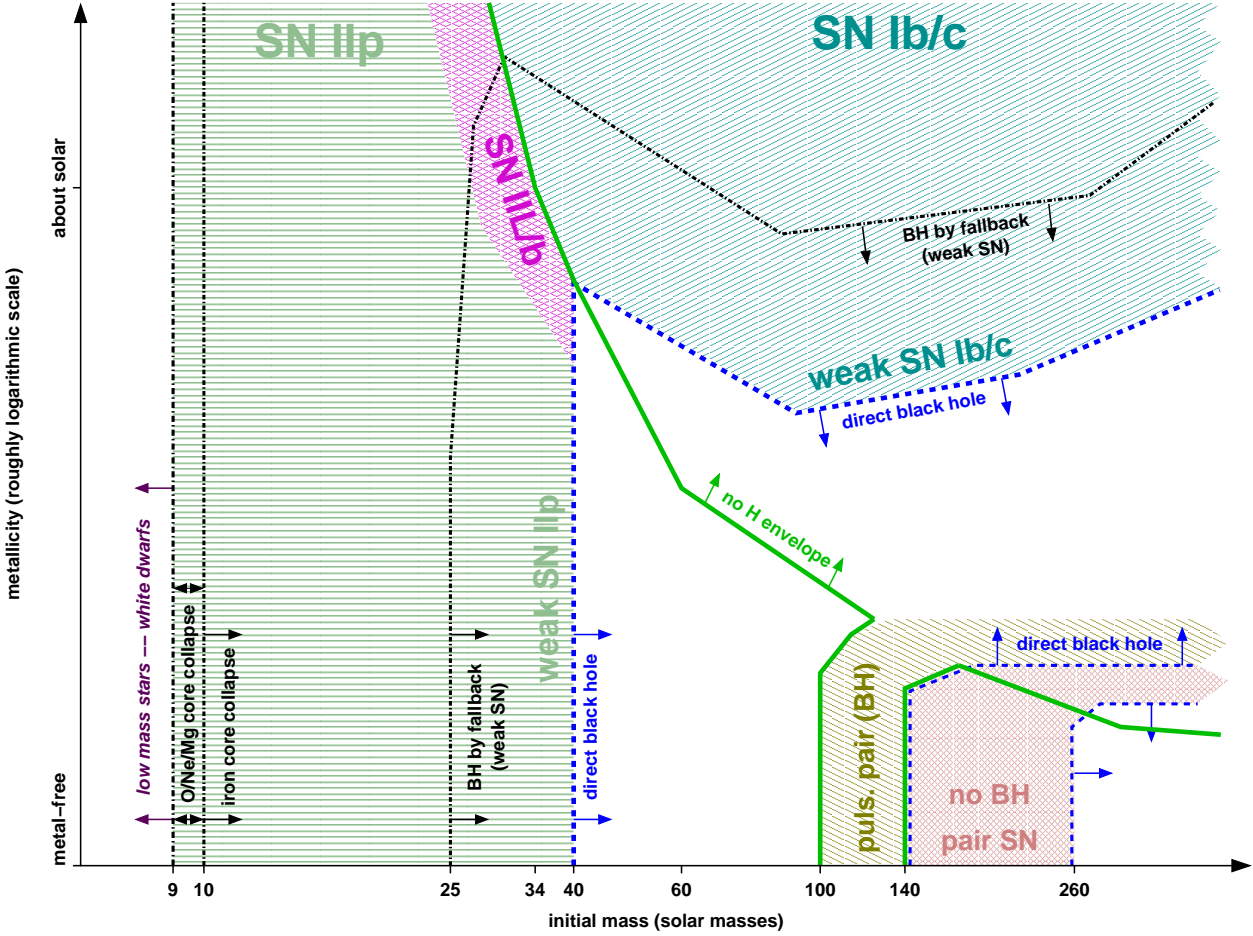


Fig. 2.— Supernovae types of non-rotating massive single stars as a function of initial metallicity and initial mass. The lines have the same meaning as in Fig. 1. Green horizontal hatching indicates the domain where Type IIP supernovae occur. At the high-mass end of the regime they may be weak and observationally faint due to fallback of  $^{56}\text{Ni}$ . These weak SN Type IIP should preferentially occur at low metallicity. At the upper right edge of the SN Type II regime, close to the green line of loss of the hydrogen envelope, Type IIL/b supernovae that have a hydrogen envelope of  $\lesssim 2 M_{\odot}$  are made (purple cross hatching). In the upper right quarter of the figure, above both the lines of hydrogen envelope loss and direct black hole formation, Type Ib/c supernovae occur; in the lower part of their regime (middle of the right half of the figure) they may be weak and observationally faint due to fallback of  $^{56}\text{Ni}$ , similar to the weak Type IIP SNe. In the direct black hole regime no “normal” (non-jet powered) supernovae occur since no SN shock is launched. An exception are pulsational pair-instability supernovae (lower right corner; brown diagonal hatching) that launch their ejection before the core collapses. Below and to the right of this we find the (non-pulsational) pair-instability supernovae (red cross hatching), making no remnant, and finally another domain where black hole are formed promptly at the lowest metallicities and highest masses (while) where nor SNe are made. White dwarfs also do not make supernovae (white strip at the very left).

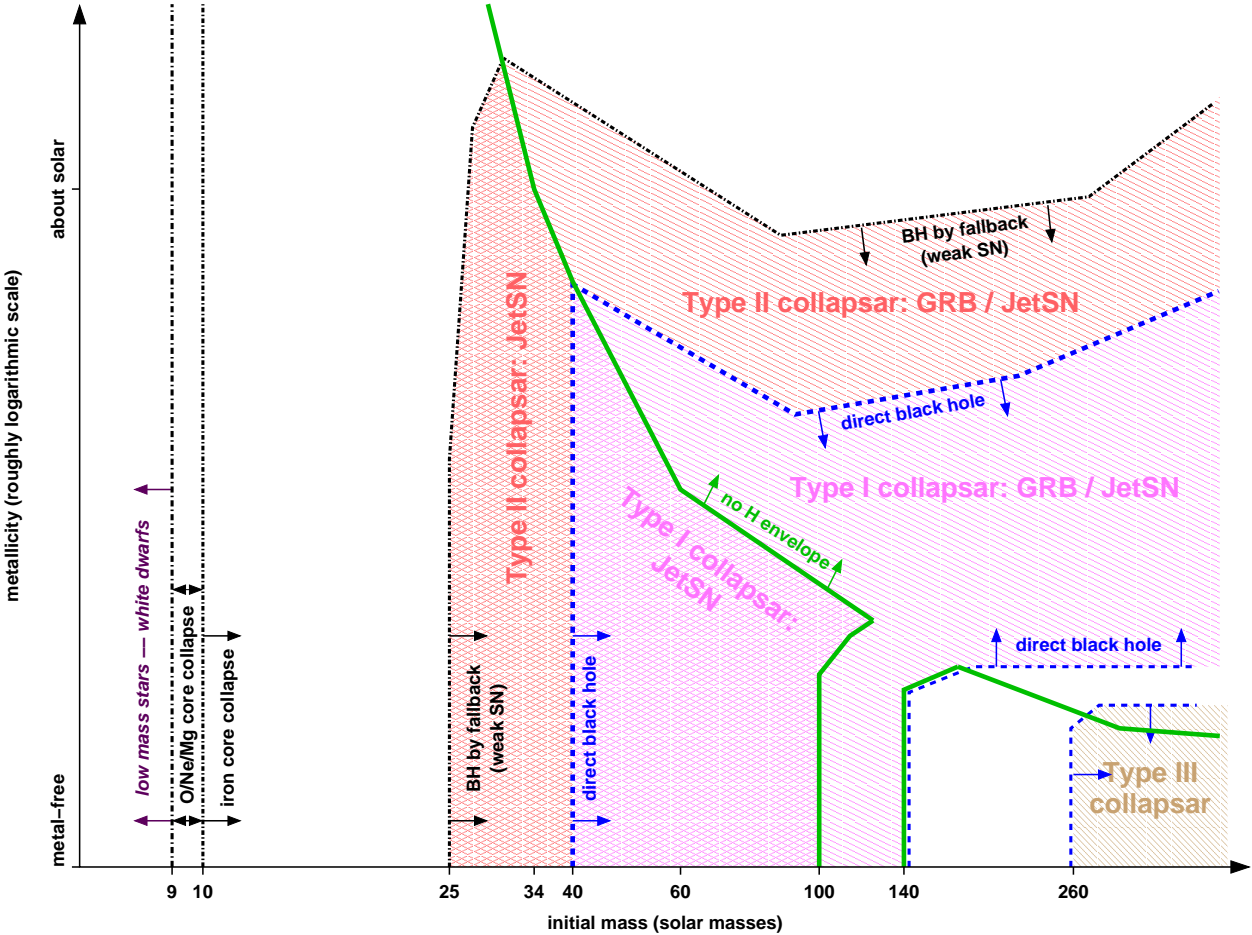


Fig. 3.— Collapsar types resulting from single massive stars as a function of initial metallicity and initial mass. Lines have the same meaning as in Fig. 1. Our main distinction is between collapsars that form from fallback (Type II; red) and directly (Type I; pink). We subdivide these into those that have a hydrogen envelope (cross hatching), only able to form jet-powered supernovae (JetSNe) and hydrogen-free collapsars (diagonal cross hatching), possibly making either JetSNe or GRBs (see also Fig. 4). The first subclass is located below the *thick green line* of loss of the hydrogen envelope and the second is above it. The *light brown diagonal hatching* at high mass and low metallicity indicates the regime of very massive black holes formed directly (Type III collapsars) that collapse on the pair-instability and photo-disintegration. Since the collapsars scenario require the formation of a BH, at low mass (left in the figure) or high metallicity (top of the figure) and in the strip of pair-instability supernovae (lower right) no collapsars occur (white).

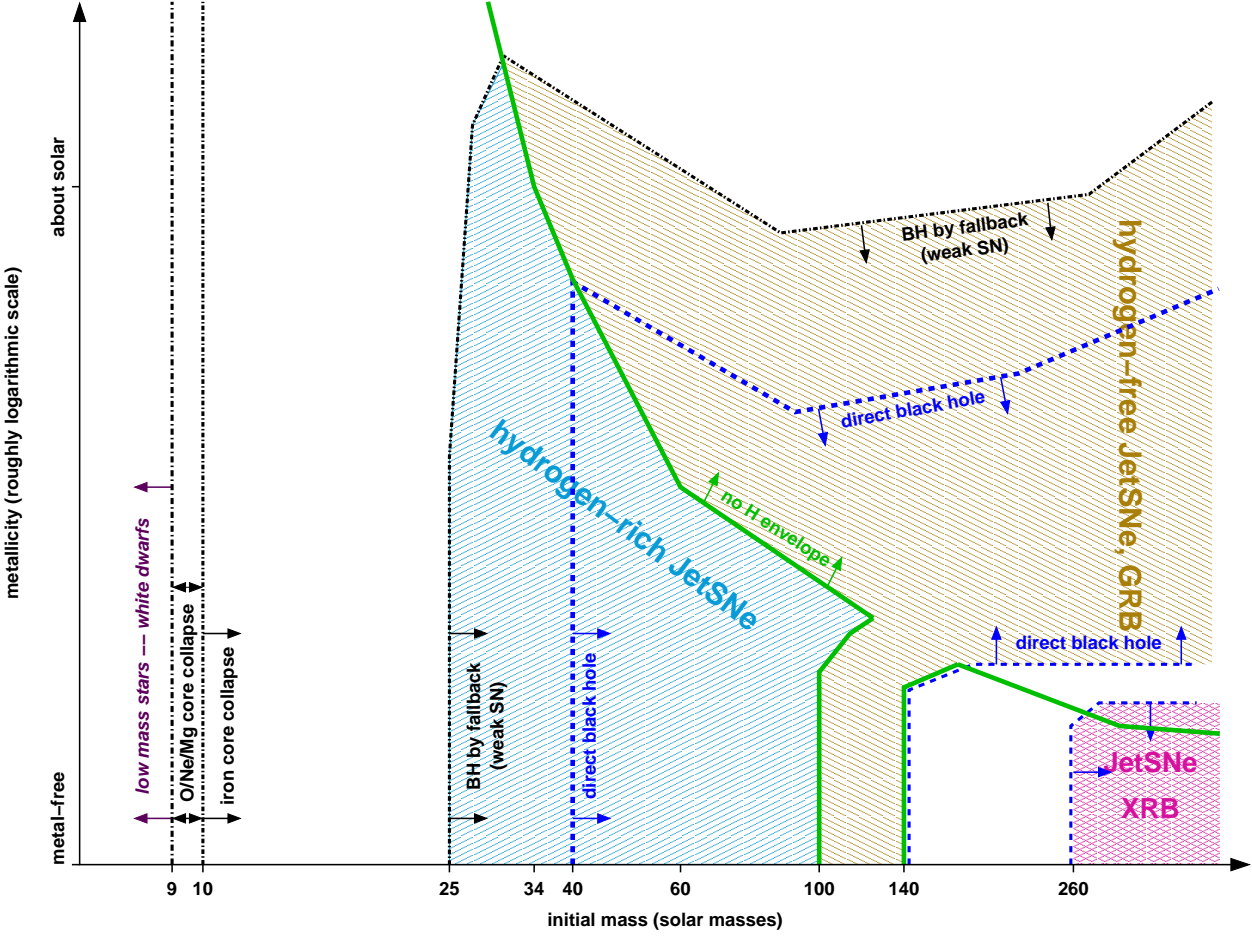


Fig. 4.— Jet-driven supernovae types as a function of initial metallicity and initial mass. Lines have the same meaning as in Fig. 1. The regimes in which hydrogen-rich JetSNe are possible (below the *thick green line* indicating loss of the hydrogen envelope) is indicated by *cyan hatching*, and that of hydrogen-free JetSNe by *light brown hatching* (above the *thick green line*). In the latter regime also GRBs may be possible, while in the first regime a hydrogen envelope is present and the travel time of a relativistic jet though it is much bigger than typical observed GRB durations. In the region of very massive black hole formation (*magenta cross hatching*; lower right corner) long JetSNe and long X-ray outbursts may occur since the bigger mass-scale of these objects also translates into a longer time-scale. If these objects are at cosmological distances, additionally the apparent time-scale and wavelength are both stretched.

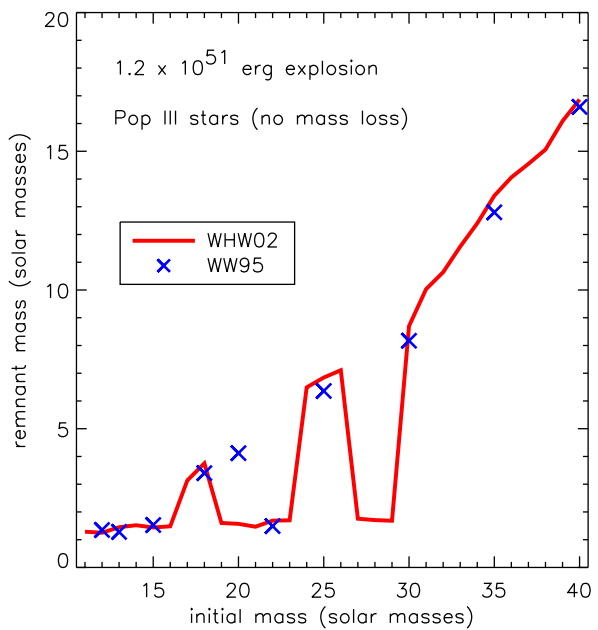


Fig. 5.— Remnant masses of metal-free stars as a function of initial mass for stars from Woosley et al. (2002, WWH02, solid line) assuming a constant kinetic energy of the ejecta of  $1.2 \times 10^{51}$  erg. The explosions were simulated by a piston at the edge of the deleptonized core similar to Woosley & Weaver (1995, WW95, crosses).

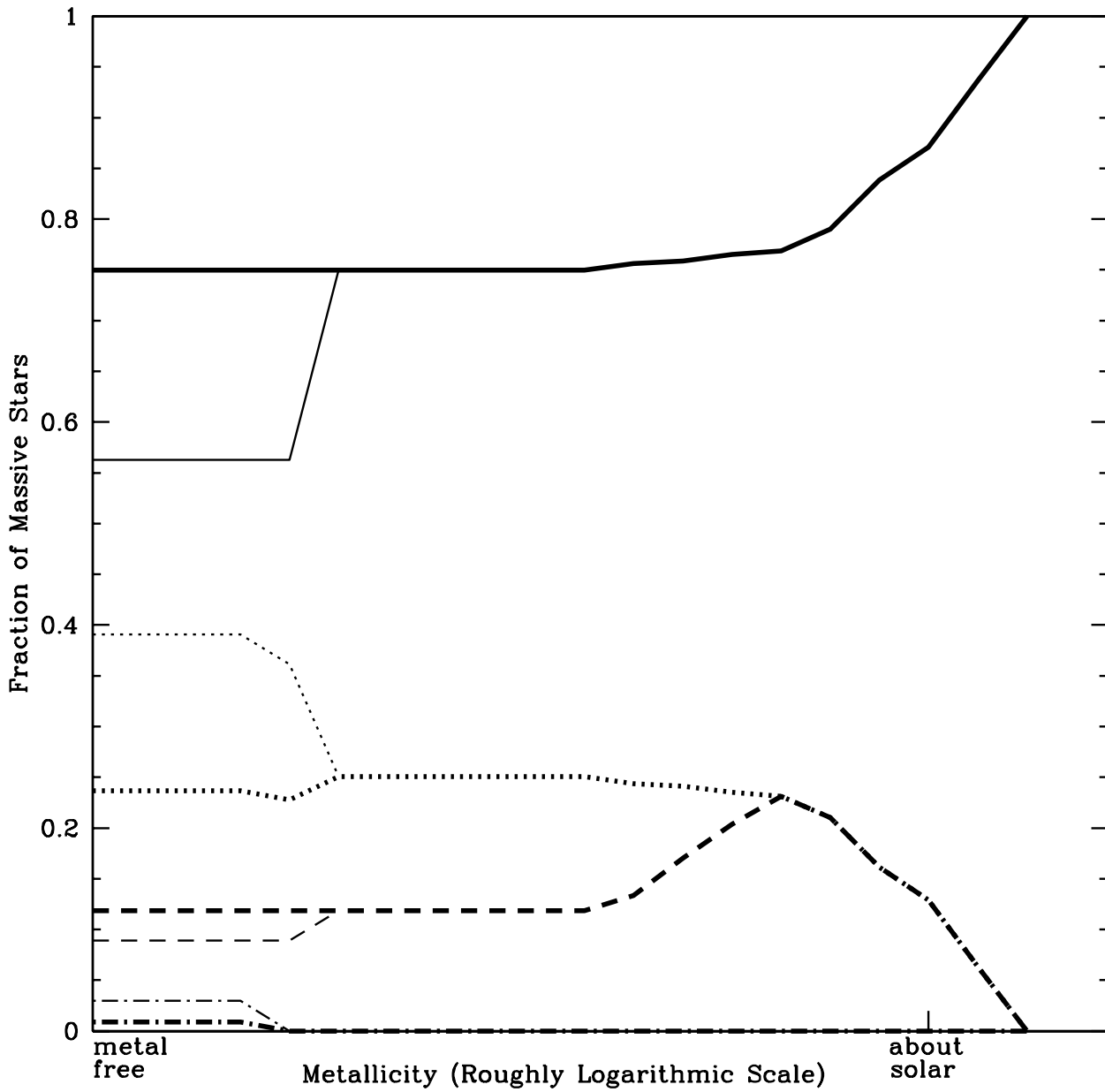


Fig. 6.— Fraction of massive stars that form neutron stars (solid line) and black holes (dotted line) as a function of metallicity for a Salpeter initial mass function (thick lines; Salpeter 1955). The dashed lines denote just those black holes formed through fallback and the dot-dashed lines denote black holes formed from very massive ( $> 300 M_{\odot}$ ) stars. The thin lines arise from assuming the IMF at low metallicity is given by Nakamura & Umemura (2001) at low metallicity (see § 5). Note that at low metallicities, pair-instability supernovae leave no compact remnant whatsoever, so that in this regime the total of all fractions is less than one.

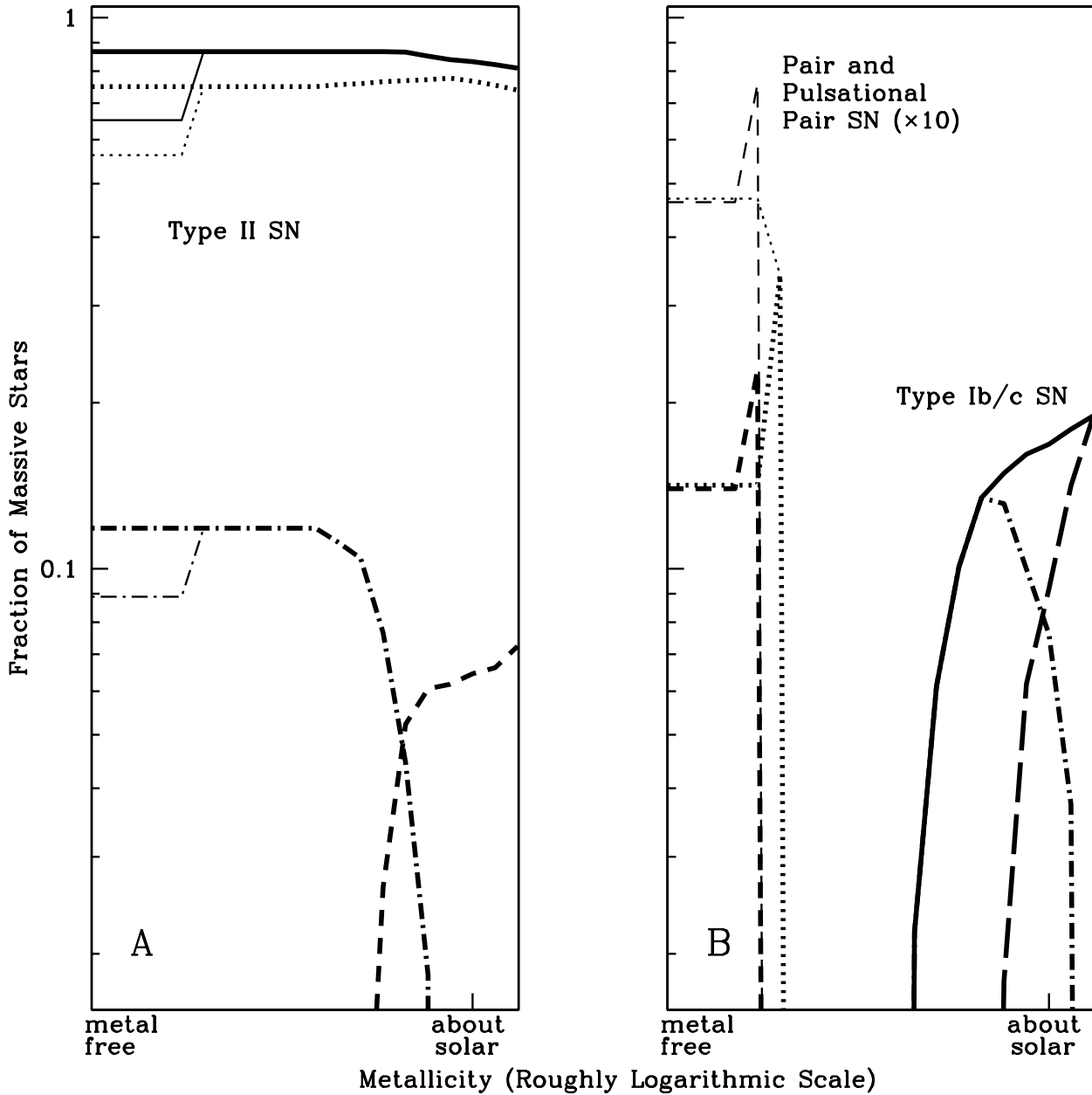


Fig. 7.— Fraction of massive stars that form supernovae for a Salpeter initial mass function (thick lines; Salpeter 1955). At low redshifts we use an alternate initial mass function (thin lines) from Nakamura & Umemura (2001). Most single stars become Type II supernovae (solid line, Panel A), and most of these are strong IIP SNe (dotted line). Roughly 15 % of Type II SNe are weak Type IIP supernovae (dot-dashed line). As the metallicity approaches solar, the fraction of weak supernovae decreases and a small fraction of Type IIL SNe are produced (dashed line). Type Ib/c supernovae are not produced until the metallicity approaches solar (solid line, Panel B), and most of these SNe will be weak (dot-dashed line). Not until the metallicity exceeds solar are strong Ib/c SNe produced (long dashed line). Pair-instability supernovae (dashed line, Panel B) and pulsational pair-instability supernovae (dotted line, Panel B) are rare and only produced at low metallicities. Their fraction depends strongly on the unknown IMF at these low metallicities. Note that in the figure we multiply the pair instability SNe fraction by a factor 10.

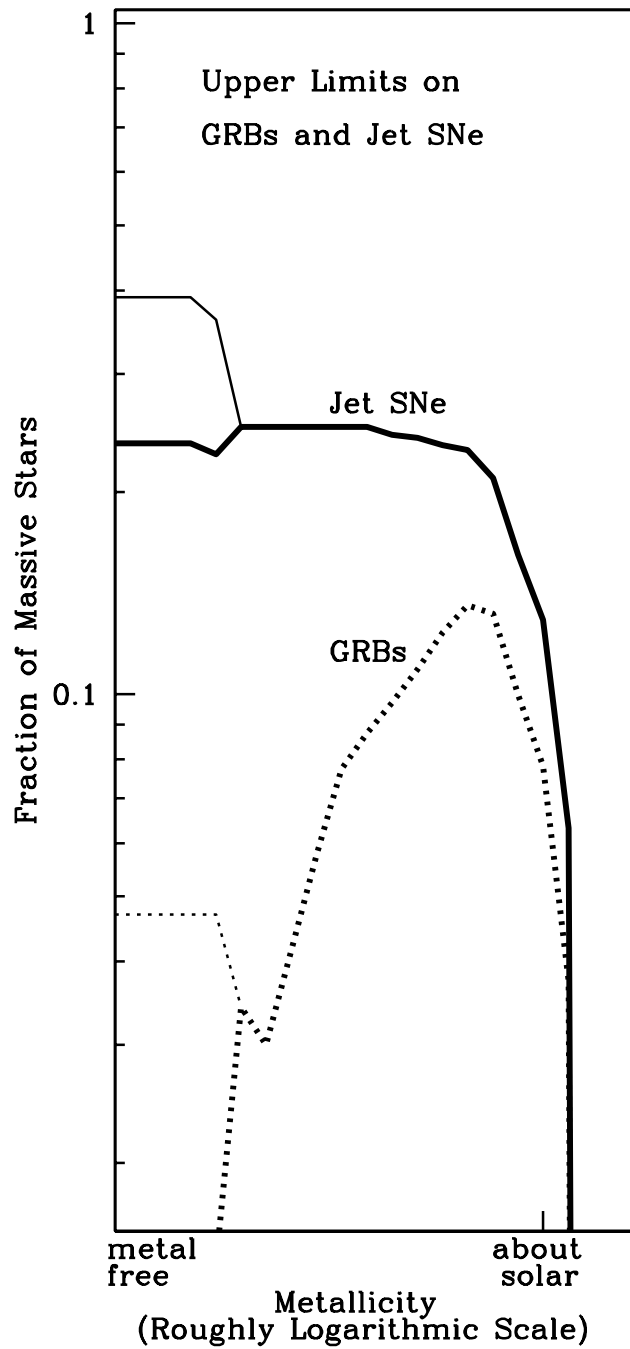


Fig. 8.— Upper limits on the fraction of massive stars that form jet-driven supernovae and gamma-ray bursts for a Salpeter initial mass function (*thick lines*; Salpeter 1955). At low redshifts we use an alternate initial mass function (*thin lines*) from Nakamura & Umemura (2001). These upper limits are determined assuming all massive stars have the necessary rotation rates to produce collapsars. Single stars produce GRBs mostly in a narrow range of metallicities, but can produce Jet SNe at all metallicities until the metallicity is so high that mass loss prohibits the formation of black holes.

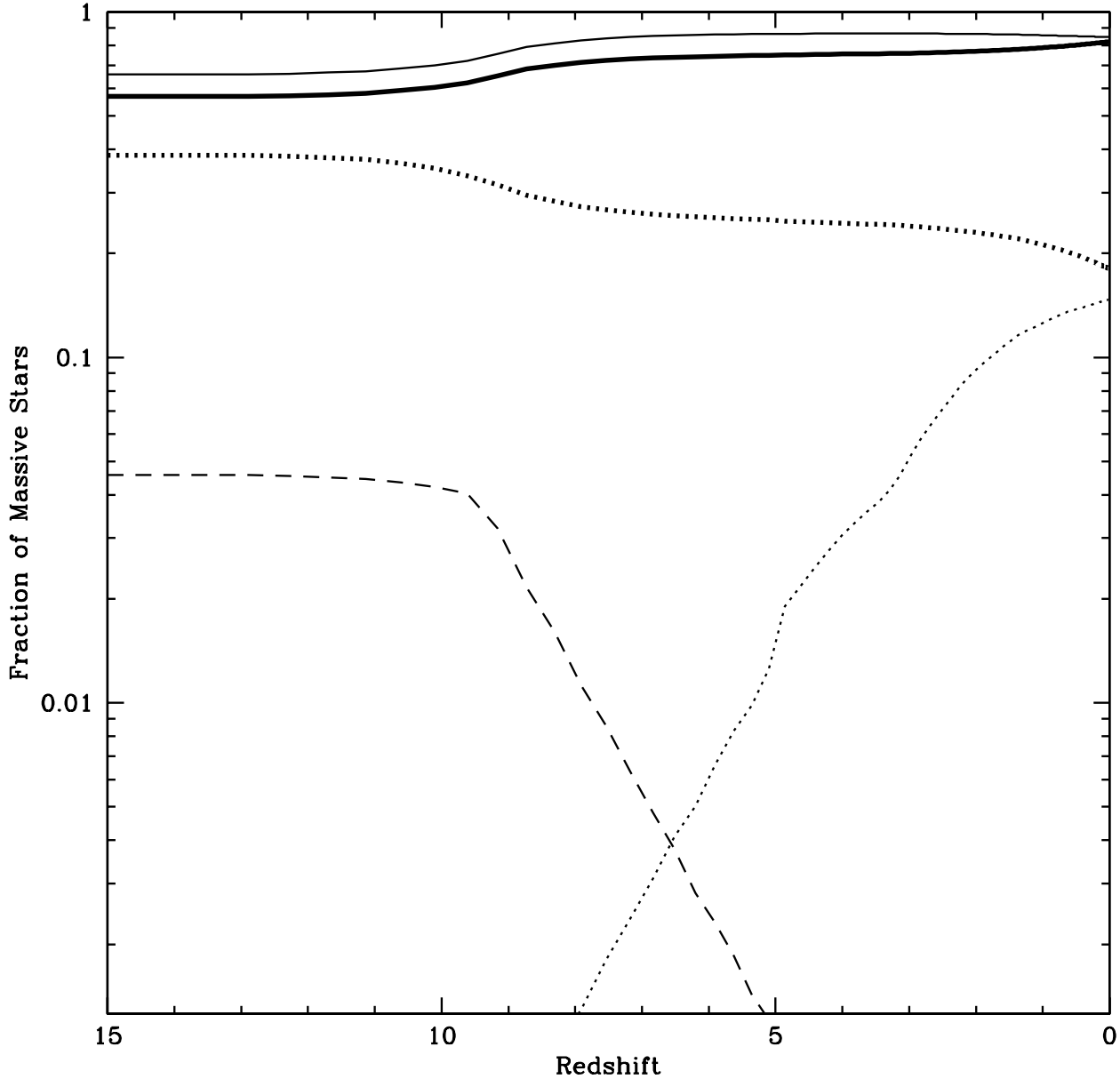


Fig. 9.— The distribution of neutron stars (thick solid line), black holes (thick dotted line), Type II SNe (thin solid line), Type Ib/c SNe (thin dotted line), pair supernovae (thin dashed line) as a function of redshift. We have assumed that the metallicity axis in Figs. 1 and 2 is indeed logarithmic with the maximum mass for which pair creation supernovae occur (Fig. 2) corresponding to a metallicity of  $10^{-4}$  solar. We have used the metallicity redshift distribution assumed by Lloyd-Ronning et al. (2002); Pei et al. (1999) distribution versus redshift with a Gaussian spread using a  $1 - \sigma$  deviation set to 0.5 in the logarithm of the metallicity. This gives an idea of the trends in the populations of massive single star outcomes as a function of redshift. Given the various assumptions that have to be made for this type of analysis, these the resulting absolute numbers should be interpreted with a great caution.